Earthquakes and Structures, *Vol. 8, No. 5 (2015) 1171-1190*
DOI: http://dx.doi.org/10.12989/eas.2015.8.5.1171

Compressive strength prediction by ANN formulation approach for CFRP confined concrete cylinders

Mojtaba Fathi[*1], Mostafa Jalal[2a] and Soghra Rostami[1b]

[1]*Department of Civil Engineering, Razi University, Kermanshah, Iran*
[2]*Zachry Department of Civil Engineering, Texas A&M University, College Station, TX 77843–3136, USA*

(Received September 28, 2014, Revised October 12, 2014, Accepted October 12, 2014)

Abstract. Enhancement of strength and ductility is the main reason for the extensive use of FRP jackets to provide external confinement to reinforced concrete columns especially in seismic areas. Therefore, numerous researches have been carried out in order to provide a better description of the behavior of FRP-confined concrete for practical design purposes. This study presents a new approach to obtain strength enhancement of CFRP (carbon fiber reinforced polymer) confined concrete cylinders by applying artificial neural networks (ANNs). The proposed ANN model is based on experimental results collected from literature. It represents the ultimate strength of concrete cylinders after CFRP confinement which is also given in explicit form in terms of geometrical and mechanical parameters. The accuracy of the proposed ANN model is quite satisfactory when compared to experimental results. Moreover, the results of the proposed ANN model are compared with five important theoretical models proposed by researchers so far and considered to be in good agreement.

Keywords: ANN formulation; CFRP confinement; concrete cylinder; strength prediction

1. Introduction

With over 50 years of excellent performance records in the aerospace industry, fiber-reinforced-polymer (FRP) composites have been introduced with confidence to the construction industry. These high-performance materials have been accepted by civil engineers and have been utilized in different construction applications such as repair and rehabilitation of existing structures as well as in new construction applications. One of the successful and most popular structural applications of FRP composites is the external strengthening, repair and ductility enhancement of reinforced concrete (RC) columns in both seismic and corrosive environments, (Hollaway 2004, Leung *et al*. 2006) .The main types of FRP composites used in external strengthening and repair of RC columns are: glass-fiber-reinforced polymers (GFRP), carbon-fiber reinforced polymers (CFRP), and aramid-fiber-reinforced polymers (AFRP). The FRP confinement can be spiral, wrapped and tube. FRP composites offer several advantages due to extremely high strength-

∗Corresponding author, Ph.D., E-mail: fathim@razi.ac.ir
[a]E-mail: m.jalal.civil@gmail.com, mjalal@tamu.edu
[b]E-mail: soghrarostami244@yahoo.com

 ISSN: 2092-7614 (Print), 2092-7622 (Online)

to-weight ratio, good corrosion behavior, electromagnetic neutrality. Thus, the effect of FRP confinement on the strength and deformation capacity of concrete columns has been extensively studied and several empirical and theoretical models have been proposed, (Nanni and Bradford 1995, Karbhari and Gao 1997, Mirmiran *et al*. 1998, Miyauchi *et al*. 1999, Saafi *et al*. 1999, Rochette and Labossiere 2000, Xiao and Wu 2000, Matthys *et al*. 2005, Lam *et al*. 2006, Deniaud and Neale 2006, Teng *et al*. 2007, Lee and Hegemier 2009).

The FRP-confined concrete is affected by unknown multivariable interrelationships and the existing experimental data are scattered; consequently, the models derived by regression analysis are not able to predict the behavior well. Meanwhile in recent years, artificial neural networks have been of interest to researchers in the modeling of various civil engineering systems among which the earlier work of the second author can be mentioned (Jalal *et al*. 2010, 2012, 2013). With this respect, this powerful tool was considered to estimate the strength enhancement of confined concrete.

This study proposes a new approach for the modeling of strength enhancement of CFRP wrapped concrete cylinders using ANNs. The proposed NN model for the compressive strength of the confined concrete cylinder is presented in explicit form.

2. Existing models of FRP-confined concrete

A variety of experimental studies (Saafi *et al*. 1999, Rochette and Labossiere 2000, Xiao and Wu 2000, Harmon and Slattery 1992, Picher *et al*. 1996, Watanabe *et al*. 1997, Kono *et al*. 1998, Toutanji 1999, Matthys *et al*. 1999, Shahawy *et al*. 2000, Micelli *et al*. 2001, Mirmiran *et al*. 1999, De Lorenzis *et al*. 2002, Dias da Silva and Santos 2001, Pessiki *et al*. 1997, Wang and Cheong 2001, Shehata *et al*. 2002, Kshirsagar *et al*. 2000, Berthet *et al*. 2005, Lin and Li 2003), performed for the description of the general behavior of FRP-confined concrete; point out a certain increase in the compressive strength of test specimens. Actually, the axial behavior of confined concrete was primarily researched by Richart *et al*. (1928), and the following well known relation was proposed for expressing the increase in the compressive strength based on their test results.

$$f'_{cc} = f'_c + k_1 f_l \tag{1}$$

where f'_{cc} is the compressive strength of confined concrete, f'_c is the compressive strength of unconfined concrete, f_l is the effective lateral confining stress, and k_1 is an experimental constant. In the literature, there are several important models, (Nanni and Bradford 1995, Karbhari and Gao 1997, Mirmiran *et al*. 1998, Miyauchi *et al*. 1999, Saafi *et al*. 1999, Rochette and Labossiere 2000, Xiao and Wu 2000, Matthys *et al*. 2005, Lam *et al*. 2006, Deniaud and Neale 2006, Teng *et al*. 2007, Lee and Hegemier 2009).

For the description of the FRP-confined concrete. The majority of such models have focused on the analytical representation of the behavior of concrete specimens with cylindrical cross section adopting the classical approach proposed by Richart *et al*. (1928). The maximum confining pressure, f_l, can be found in usual way as

$$f_l = \frac{2ntE_{frp}\varepsilon_{rup}}{d} \tag{2}$$

Where, E_{FRP} represents the tensile modulus of FRP composite, t is the thickness of the

Table 1 Some of the important strength models for FRP-confined concrete

Author	Formula	Type
Lam and Teng	$f'_{cc}/f'_c = 1 + 2\dfrac{f_l}{f'_c}$	linear
Xiao and Wu	$f'_{cc}/f'_c = 1.1 + (4.1 - 0.75\dfrac{f'^2_c}{E_l})\dfrac{f_l}{f'_c}$	second-order
Saafi *et al.*	$f'_{cc}/f'_c = 1 + 2.2(\dfrac{f_l}{f'_c})^{0.84}$	nonlinear
Samaan *et al.*	$f'_{cc}/f'_c = 1 + 6.0\dfrac{f_l^{0.7}}{f'_c}$	nonlinear
Saadatmanesh *et al.*	$f'_{cc}/f'_c = 2.254(1 + 7.94\dfrac{f_l}{f'_c})^{0.5} - 2\dfrac{f_l}{f'_c} - 1.254$	second-order

composite jacket, ε_{rup} is the ultimate circumferential strain in the composite jacket and d is the diameter of the concrete core.

After this approach, many researchers investigated specifically the FRP-confined concrete and consequently a considerable number of models developed. All of the proposed models were developed empirically by either doing regression analysis using existing test data or by a development based on the theory of plasticity with four or five parameters to be determined using available experimental data. The existing models can be classified into three major categories including linear, second-order and nonlinear models. Table 1 presents some important existing empirical models to predict the compressive strength of FRP-confined concrete.

In this study, an ANN approach has been presented to estimate strength enhancement of confined concrete. Compressive strength values of 128 concrete cylinders confined with CFRP composite jackets tested by several researchers (Saafi *et al*. 1999, Rochette and Labossiere 2000, Xiao and Wu 2000, Harmon and Slattery 1992, Picher *et al*. 1996, Watanabe *et al*. 1997, Kono *et al*. 1998, Toutanji 1999, Matthys *et al*. 1999, Shahawy *et al*. 2000, Micelli *et al*. 2001, Mirmiran *et al*. 1999, De Lorenzis *et al*. 2002, Dias da Silva and Santos 2001, Pessiki *et al*. 1997, Wang and Cheong 2001, Shehata *et al.* 2002, Kshirsagar *et al*. 2000, Berthet *et al*. 2005, Lin and Li 2003) are compared with the predictions of the existing five analytical models (Saafi *et al*. 1999, Xiao and Wu 2000, Saadatmanesh *et al*. 1994, Samaan *et al*. 1998, Lam and Teng 2002) and the ANN model.

3. Artificial neural networks

From historical point of view, neural networks appear to be a recent development. However, this field was established before the advent of computers. An artificial neural network (ANN) is an information processing tool that is inspired by the way biological nervous systems (such as the brain), process the information. The key element of this tool is the novel structure of the information processing system. It is composed of a large number of highly interconnected processing elements (called neurons) working in unison to solve specific problems. Similar to human, ANNs learn by examples. An ANN is configured for a specific application, such as pattern

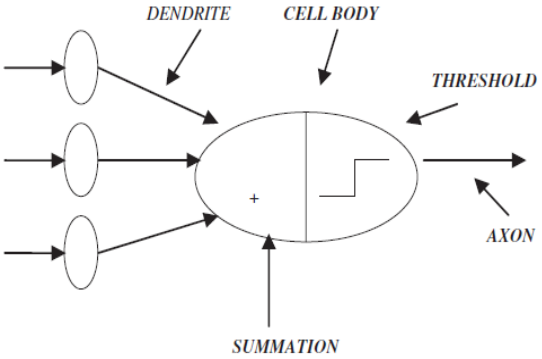

Fig. 1 Schematic of a neuron and its components

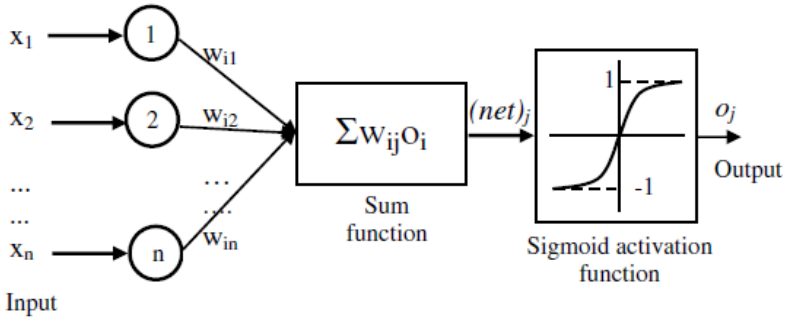

Fig. 2 Artificial neuron model

recognition or data classification, through a learning process. Learning in biological systems involves adjustments to the synaptic connections that exist between the neurons; the same process happens in ANNs. Artificial neural networks provide a general practical method for real-valued, discrete-valued, and vector-valued functions from examples and so they have been widely used in the various applications of engineering fields. In engineering applications, a neural network can be a vector mapper which maps an input vector to an output one.

Regarding the neural network architectures, a single biological neuron is composed of three major parts including the cell body, the axon, and the dendrite. Fig. 1 shows the schematic drawing of representative biological neurons and a simplified computational neuron. The cell body of a neuron is connected to the dendrite of a neighboring neuron.

These individual biological neurons are interconnected with the other neurons through hair-like dendrites. A group of these neurons can consist of layers of neurons, and a collection of layers can form nerve systems in the human body. Signal communications between neurons are continuously generated which is delivered from one neuron to the others by firing an electrical signal generated through a chemical reaction. The other neurons receive the signal through the interfaces with the neighboring neurons, referred to as a synapse. This system is capable of learning, recalling, and generating output corresponding to external signals. If a system of neurons has a consistent and frequent external signal, its output signal will be consistent and thus stored in the system. On the other hand, if it is subjected to an insistent or rare signal, the memory for this type of information may vanish after receiving other signals or patterns. This biological neuron system can work

collectively to handle more complicated learning to illustrate how the mathematical operations are used to mimic the major biological functionalities. The general computational neuron is shown in Fig. 2. Similar to biological neurons, a computational neuron has input, a neuron cell, and output. Each neuron is commonly connected with net-like internal weights in which complex knowledge is embedded. The ANN types can be distinguished by overall structure, neuron type, training data space, and learning rules among others. Each input is weighted with an appropriate w. The sum of the weighted inputs and the bias forms the input to the transfer function *f*. Neurons can use any differentiable transfer function f to generate their output.

Back propagation is the generalization of the Widrow-Hoff learning rule to multiple-layer networks and nonlinear differentiable transfer functions. Since networks with biases, a sigmoid layer, and a linear output layer are capable of approximating any function with a finite number of discontinuities, input vectors and the corresponding target vectors are used to train a network until it can approximate a function. The most common backpropagation training algorithm is Levenberg-Marquardt which was used in this investigation.

4. Neural network modeling

As the first step for providing sufficient information for training, verifying and testing of neural networks, a comprehensive set of test results on the axial compressive strength of CFRP-confined cylindrical concrete specimens was collected. All together, the selected database contains 128 test results including significant test programs of three recent decades (Saafi *et al*. 1999, Rochette and Labossiere 2000, Xiao and Wu 2000, Harmon and Slattery 1992, Picher *et al*. 1996, Watanabe *et al*. 1997, Kono *et al*. 1998, Toutanji 1999, Matthys *et al*. 1999, Shahawy *et al.* 2000, Micelli *et al*. 2001, Mirmiran *et al*. 1999, De Lorenzis *et al*. 2002, Dias da Silva and Santos 2001, Pessiki *et al*. 1997, Wang and Cheong 2001, Shehata *et al*. 2002, Kshirsagar *et al*. 2000, Berthet *et al*. 2005, Lin and Li 2003). It is worth mentioning that FRP rupture has been the failure mode for all the specimens of the test programs used in this research. The six input parameters were determined based on physical considerations, as well as the observed trend of failure mode reported by tests on the axial compressive strength of cylindrical concrete specimens confined by CFRP. From the test results and also the general form for many of existing strength models, Eq. (1), it can be concluded that the compressive strength of confined concrete is definitely affected by the compressive strength of the unconfined concrete (f'_c), the lateral confining strength, Eq. (2), including the ultimate circumferential strain in the FRP jacket (ε_{rup}), the total thickness of FRP (t) and the diameter of the cylindrical concrete specimen (d). The input of specimen height (h) as a separate parameter is also necessary in order to take into account the effect of the length-to-diameter ratio (h/d) of the specimens which is considered by some researchers in their empirical models. Finally, the elastic modulus of FRP (E_{FRP}) was selected as the last input parameter since its effect on f'_{cc} has been considered in some existing models such as formula proposed by Karbhari and Gao (1997).

Among six input parameters, only thickness of FRP could be replaced by combination of layers number and thickness of each layer based on available empirical models and this investigation. However, using layers number instead of total thickness requires each layer thickness to be determined and consequently one additional parameter and correction factor would appear in the proposed model. Since the majority of test results only present the total thickness of FRP and also

there is a clear need to develop a simple model having least possible number of input parameters, the total thickness of FRP (t) was only considered in training the networks. So the parameters used as the input nodes in the ANN modeling are summarized as:

-d (mm): Diameter of the cylindrical concrete specimen
-h (mm): Height of the cylindrical concrete specimen
-t (mm): Total thickness of CFRP jacket
-ε_{rup} (mm): Ultimate circumferential strain in the CFRP jacket
-E_{FRP} (MPa): Elastic modulus of CFRP
-f'_c (MPa): Compressive strength of the unconfined concrete

Having the six input nodes as described above, the target node was the compressive strength of the confined concrete (f'_{cc}). One hidden layer was used in this ANN modeling, where transfer functions were log-sigmoid. Before training the selected data, normalization/ scaling for the whole data were made. This was done since log-sigmoid transfer function was used in the network which recognizes values between 0 and 1. In order to scale the data from 0.1 to 0.9, minimum and maximum values were taken to use linear relationship between those values. Statistical properties for scaling the input parameters are listed in Table 2 and Eq. (3) shows the scaling equation.

$$X_{scaled} = (0.9-0.1)\frac{X - X_{\min}}{X_{\max} - X_{\min}} + 0.1 \tag{3}$$

Where X is an input parameter, $X_{\min}$ and $X_{\max}$ are minimum and maximum values of the input parameter respectively, and X_{scaled} is the scaled value of the input parameter between 0 and 1.

Levenberg-Marquardt (LM) algorithm randomly divides input vectors and target vectors into three sets including training, validation and testing. Changing the relative percentages of these three sets could slightly improve the generalization process. In this study, as a preliminary step, some data sets with different relative percentages were examined in which the training data varies from 50% to 90% and the values of 60%, 20%, and 20% was selected for training, validation and testing respectively in order to obtain the most efficient distribution of data sets. So, 60% of whole data was specified as the training data in which the network would be adjusted according to its error. Similarly 20% of database was considered as the validating data which was used to measure network generalization and to halt training when generalization stops improving. Finally, the remaining 20% of whole data was specified as the testing data which has no effect on training and so provides an independent measure of network performance during and after training.

The network architecture used in this study was called NN 6-n-1, where the first digit is the number of input nodes, n is the number of hidden nodes and third digit is the number of output nodes as shown in Fig. 3.

Table 2 Statistical properties of experimental data

Input parameters	d (mm)	h (mm)	t (mm)	E_{frp} (MPa)	ε_{rup} (mm)	f'_c (MPa)	f'_{cc} (MPa)
Mean	131.19	294.81	0.41	211221.60	0.0091	39.68	77.51
Max	200	610	2	611600	0.0207	171	303
Min	51	102	0.0890	19900	0.0017	17.39	31.40
Standard deviation	34.98	120.86	0.36	108110.51	0.0033	25.61	43.54
Coefficient of variation	0.41	0.26	0.88	0.51	0.36	0.64	0.56

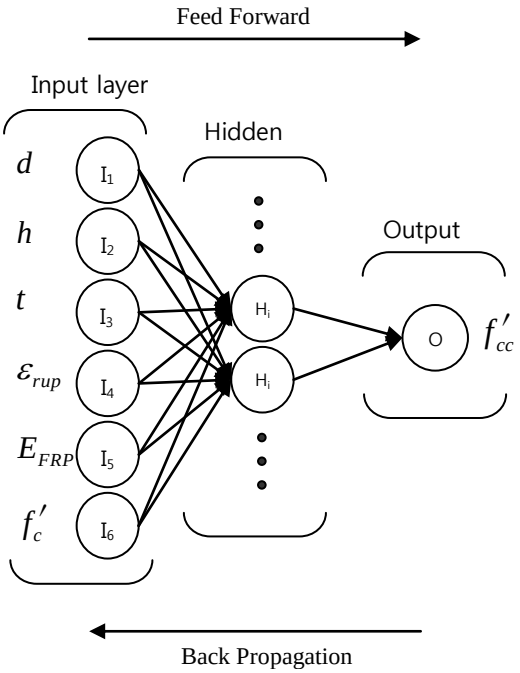

Fig. 3 Schematic diagram of ANN model

4.1 Optimal NN model selection

The performance of an NN model mainly depends on the network architecture and parameter settings. One of the most difficult tasks in NN studies is to find this optimal network architecture which is based on determination of numbers of optimal layers and neurons in the hidden layers by trial and error approach. The assignment of initial weights and other related parameters may also influence the performance of the NN in a great extent. However, there is no well-defined rule or procedure to have optimal network architecture and parameter settings where trial and error method still remains valid.

The criterion for stopping the training of the networks was Mean Square Error (MSE) which is the average squared difference between outputs and targets. Lower values mean better performance of the network (zero means no error). Regression values (*R*-values) measure the correlation between outputs and targets in the networks; An *R*-value of 1 means a close relationship and in contrast, 0 means a random relationship. These two criteria (MSE and *R*-values) were considered as the basis for selecting the idealized network. The mean square error values and the averages for 10 trials of each network with n hidden neurons are presented in Figs. 4 and 5 respectively.

The two lowest MSE trends are presented in boldface lines. Another filtering in the pre-elimination of networks can be seen in Fig. 6, where the regression values of the networks were noted. It can be seen that all the networks were trained well, but some of them resulted large values of Mean Square Error (MSE).

After the pre-acceptance of desirable networks with lower mean square error according to Fig. 4,

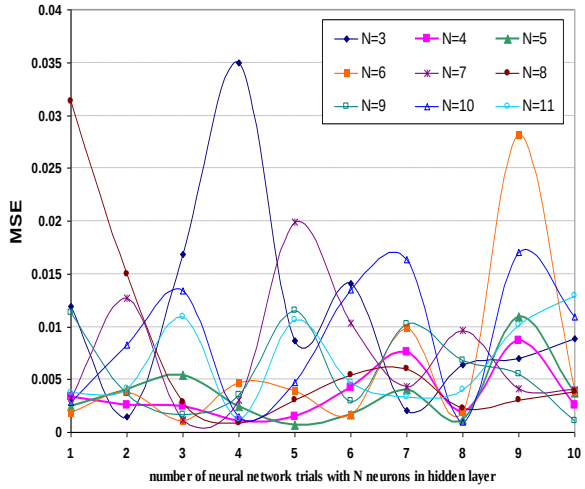

Fig. 4 MSE trends for 10 trials of NN 6-n-1

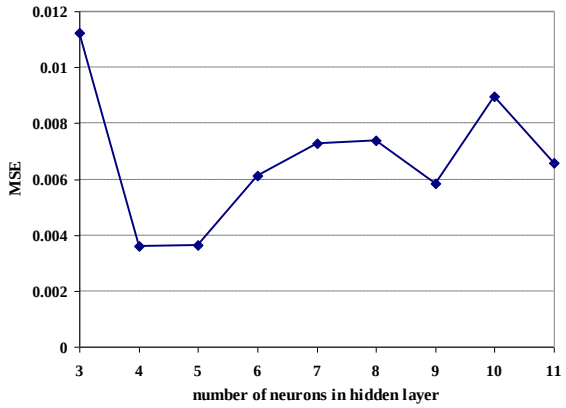

Fig. 5 Average of mean square error for 10 trials of each NN 6-n-1

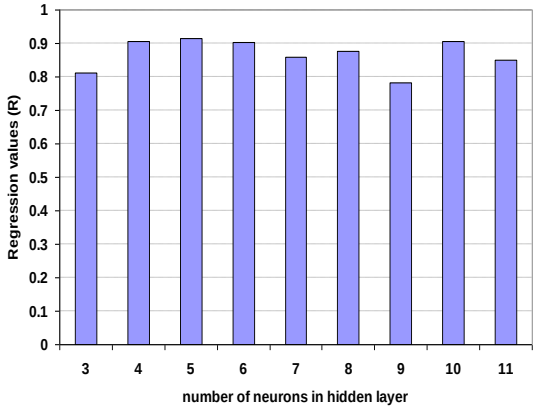

Fig. 6 Average of R values for 10 trials of each NN 6-n-1

the best networks are: NN 6-4-1 and NN 6-5-1. In order to arrive at a single ideal model, NN 6-5-1 was chosen since it presents good results with respect to the least value of MSE and the maximum R-values among all networks.

5. Results of NN model

The experimental database is randomly divided as training, validation and test sets. As mentioned before, about 76, 52 and 52 data sets among all were used for training, validation and testing respectively. The prediction of NN and actual values of learning, validation, testing and all data sets and their corresponding correlation are given in Figs. 7-10.

Fig. 11 shows the mean squared error of the network starting at a large value and decreasing to a smaller value. In other words, it shows that the network is learning. The plot has three lines,

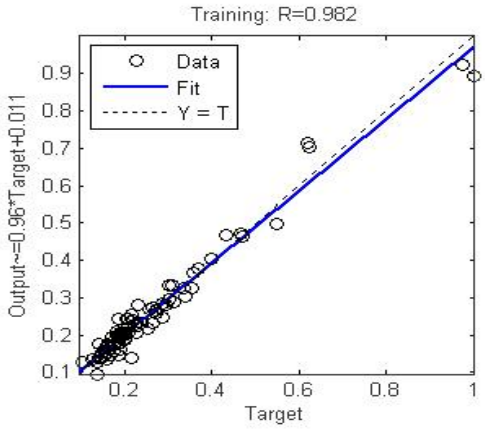

Fig. 7 Regression of training data simulated by NN 6-5-1

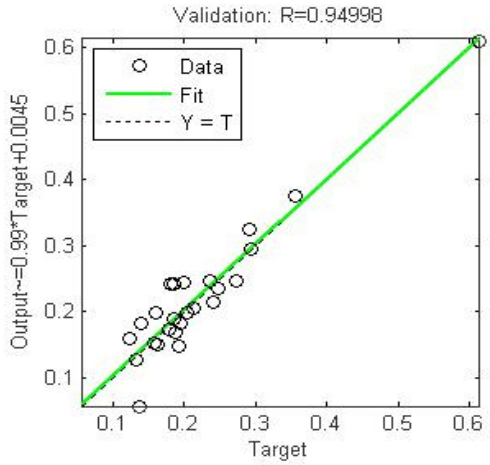

Fig. 8 Regression of validation data simulated by NN 6-5-1

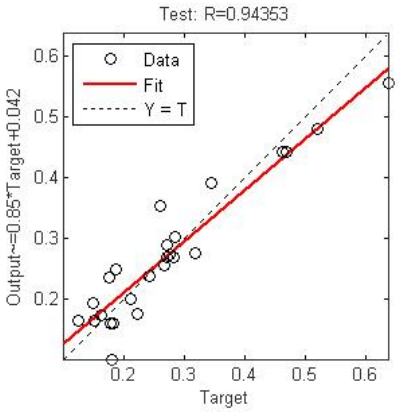

Fig. 9 Regression of test data simulated by NN 6-5-1

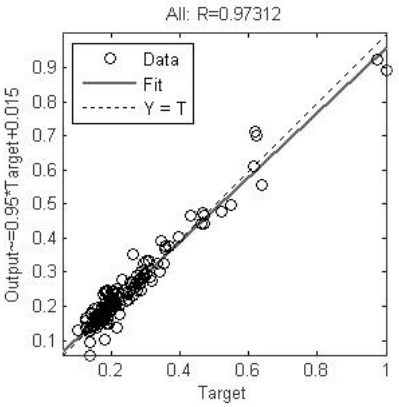

Fig. 10 Regression of total data simulated by NN 6-5-1

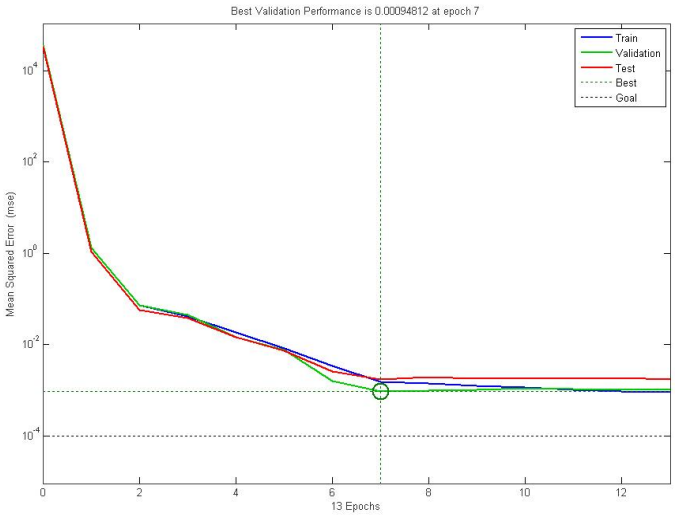

Fig. 11 Performance of NN 6-5-1 for MSE of train, validation and test after 13 epochs

because the 128 input and targets vectors are randomly divided into three sets. Training on the training vectors continues as long as the training reduces the network's error on the validation vectors. After the network memorizes the training set (at the expense of generalizing more poorly), training is stopped. This technique automatically avoids the problem of over-fitting, which plagues many optimization and learning algorithms.

5.1 Comparison of ANN with empirical models

The five existing analytical models for verification of the ANN model selected including the strength models proposed by Lam and Teng (2002) as a linear model, Saafi *et al*. (1999), Samaan *et al*. (1998) as nonlinear models, Xiao and Wu (2000), Saadatmanesh *et al*. (1994) as second-order models, are listed in Table 1. The simulated compressive strengths of the CFRP-confined concrete from idealized neural network compared to the five existing strength models and

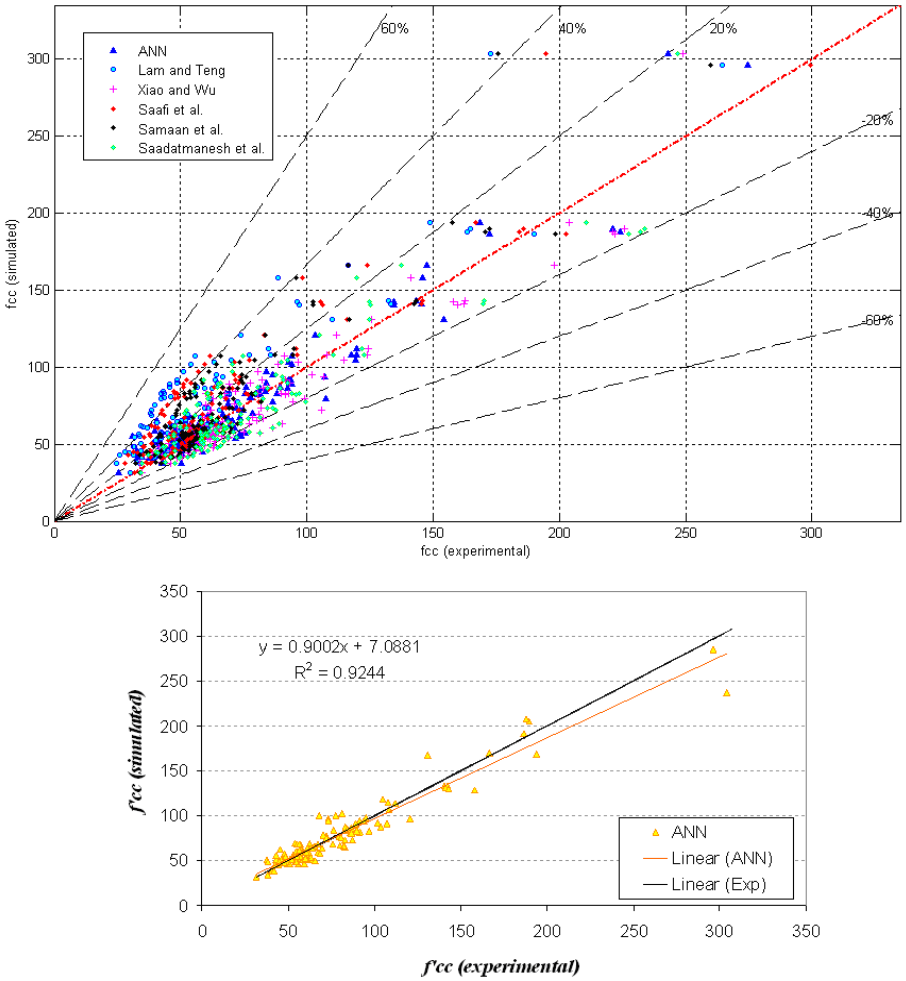

Fig. 12 Comparison of various predicted values of f'_{cc} and correlation between ANN results and experimental data

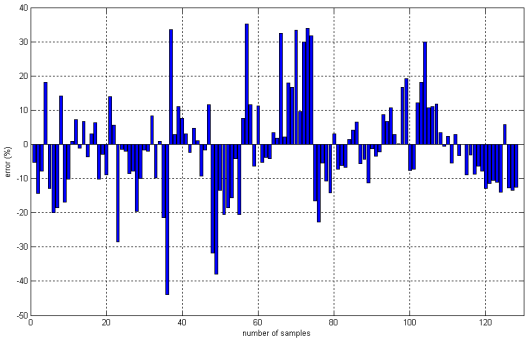

Fig. 13 Prediction errors of NN model

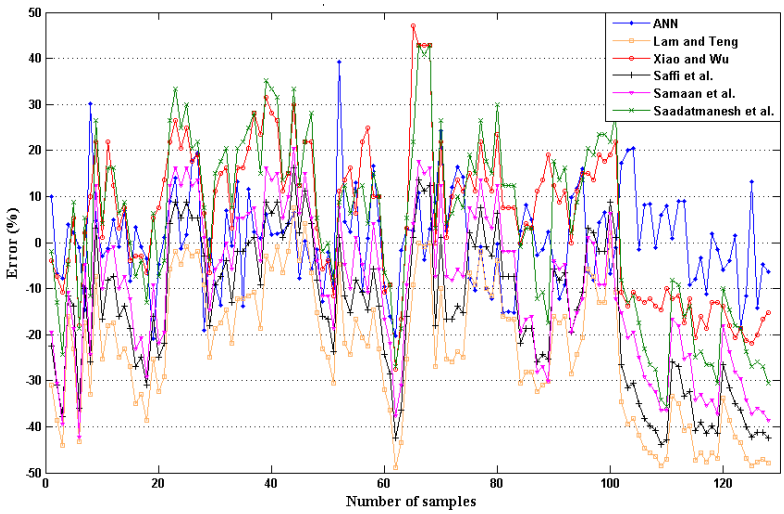

Fig. 14 Comparison of prediction errors for all models

correlation between ANN results and experimental data are plotted in Fig. 12. If there is perfect agreement between the model and experimental results, all the points will lie along the diagonal. The predictions errors (%) of ANN and other five models are presented in Figs. 13 and 14.

6. Explicit formulation of the NN model

As it was indicated in the previous section, the simulated results from the neural network are in reasonably good agreement with the experimental data. But it is not convenient to use the network in engineering design since the network contains many weights and biases together with transfer functions and consequently the final equations will become very complicated. In order to come up with this problem, the neural network should be employed to generate empirical design curves and equations for use in design. The range and reference value for each of the six input parameters are first chosen to be close to their mean values and are presented in Table 3.

Table 3 Range of input parameters and their corresponding reference values used in derivation of empirical design approach

Input Parameters	d (mm)	h (mm)	t (mm)	E_{frp} (MPa)	ε_{rup} (mm)	$f'c$ (MPa)
Max	200	610	2	611600	0.0207	171
Min	51	102	0.0890	19900	0.0017	17.39
Reference	130	300	0.5	211000	0.009	40

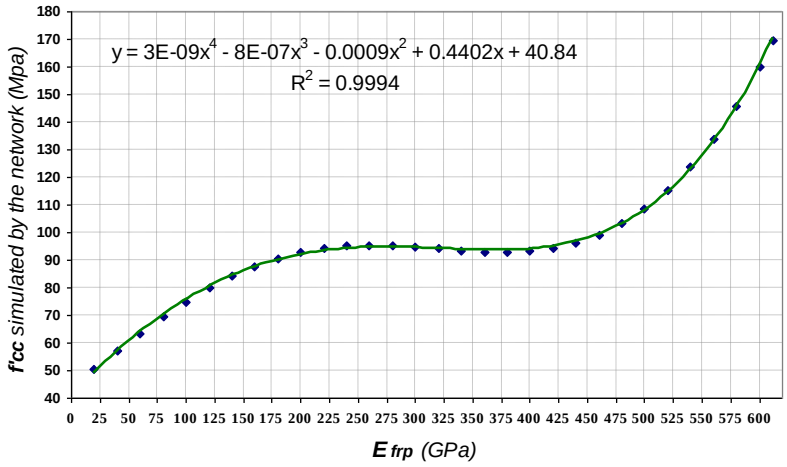

Fig. 15 Variations of f'_{cc} against E_{FRP} assuming other input parameters to be in their reference value

The pattern formula used here for predicting the compressive strength of CFRP-confined concrete was introduced by Leung *et al*. (2006), for determining ultimate FRP strain of FRP-strengthened concrete beams. This pattern with a little modification in using an equation instead of the f'_{cc} vs. E_{FRP} curve itself, has been used herein. As the first step, f'_{cc} is first plotted against E_{frp} in Fig. 15 assuming the other five input parameters to be kept constant at their respective reference values. The relationship that quite fits the curve is given in Eq. (4).

$$f'_{cc}(E_{frp}) = 3\times10^{-9}(E_{frp})^4 - 8\times10^{-7}(E_{frp})^3 - 0.0009(E_{frp})^2 + 0.4402(E_{frp}) + 40.84 \quad (4)$$

To account for the effect of five other parameters on f'_{cc}, a correction function has to be derived. The correction function can be written in the following form

$$F(d,h,t,\varepsilon_{rup},f'_c) = C(h)\times C(d)\times C(t)\times C(\varepsilon_{rup})\times C(f'_c) \quad (5)$$

According to Eq. (5), the variation of f'_{cc} with each parameter is assumed to be independent of the other parameters. The correction factor $C(h)$, for example will be derived to show the derivation procedure of correction factors. To derive $C(h)$, master curves are first obtained with different d values, but with h fixed at the reference value of 300. For each combination of h and d, f'_{cc} is obtained from the neural network. The number of vectors to draw the correction factors was

chosen to be about 25% of whole data which is approximately equal to 30 data sets. By dividing the network simulated value by the value obtained from the master curves, the correction factor $C(h)$ can be obtained.

In Fig. 16, $C(h)$ is plotted against h for various values of d. the same process was performed to plot $C(h)$ against variations of other input parameters including t, ε_{rup} and f'_c (Figs. 17-19).

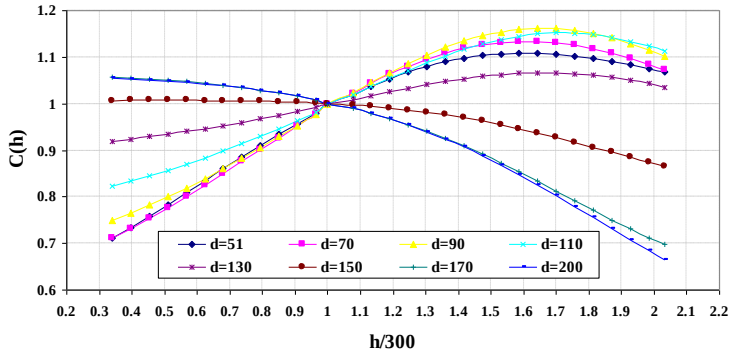

Fig. 16 Correction factor $C(h)$ with various values of d

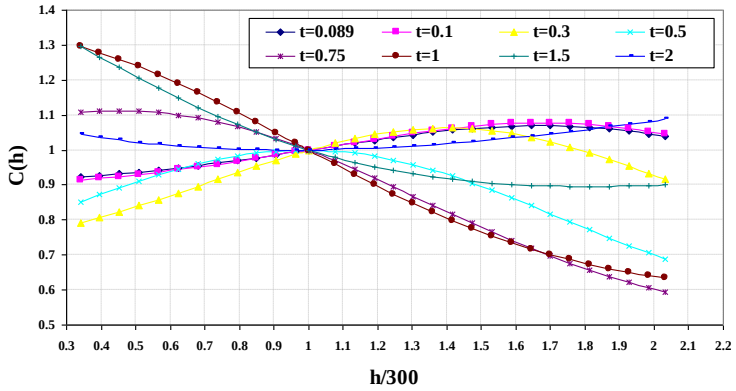

Fig. 17 Correction factor $C(h)$ with various values of t

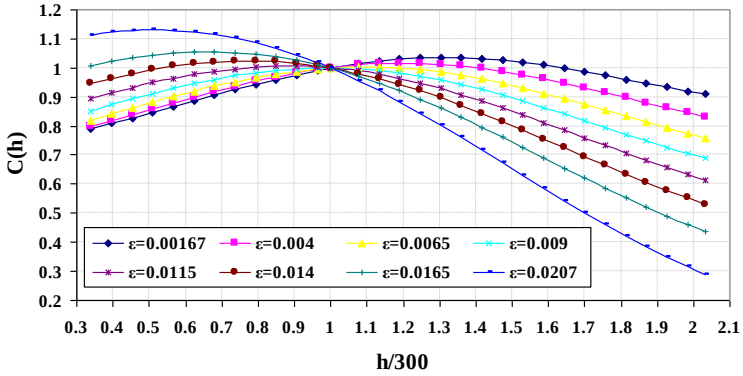

Fig. 18 Correction factor $C(h)$ with various values of ε_{rup}

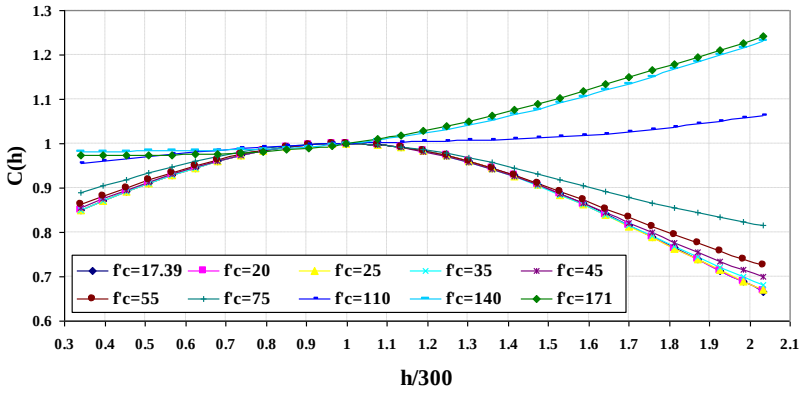

Fig. 19 Correction factor $C(h)$ with various values of f'_c

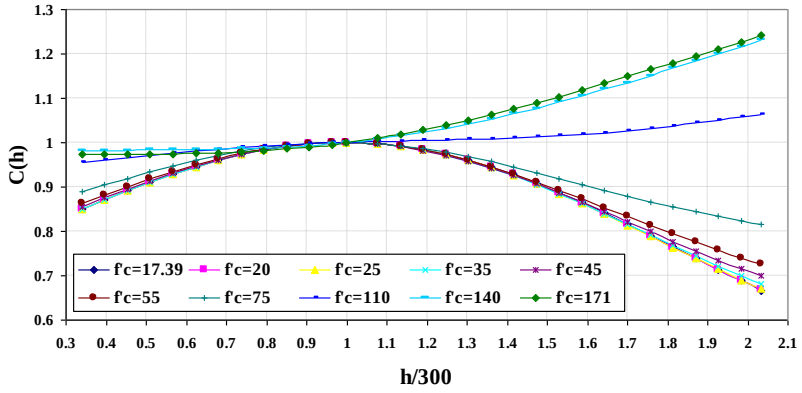

Fig. 20 All data of $C(h)$ and the best fitting curve

By considering all curves for $C(h)$, a line that fits the curve with the best correlation and minimum least square error was found as shown in Fig. 20. The same procedure has been applied to obtain the equations of correction factors for the other input parameters (Figs. 21-24)

$$C(h) = 0.0665\left(\frac{h}{300}\right)^4 - 0.2904\left(\frac{h}{300}\right)^3 + 0.2598\left(\frac{h}{300}\right)^2 + 0.0895\left(\frac{h}{300}\right) + 0.8739 \tag{6}$$

$$C(d) = 4.1001\left(\frac{d}{130}\right)^4 - 13.086\left(\frac{d}{130}\right)^3 + 16.781\left(\frac{d}{130}\right)^2 - 10.779\left(\frac{d}{130}\right) + 3.9514 \tag{7}$$

$$C(t) = 0.991(t/0.5)^{0.3631} \tag{8}$$

$$C(\varepsilon_{rup}) = 0.0267\left(\frac{\varepsilon_{rup}}{0.009}\right)^5 - 0.1082\left(\frac{\varepsilon_{rup}}{0.009}\right)^4 + 0.0855\left(\frac{\varepsilon_{rup}}{0.009}\right)^2 + 0.025\left(\frac{\varepsilon_{rup}}{0.009}\right) + 0.0475\left(\frac{\varepsilon_{rup}}{0.009}\right) + 0.9236 \tag{9}$$

$$C(f'_c) = 0.6593\, e^{0.3521(f'_c/40)} \tag{10}$$

Consequently, the compressive strength of CFRP-confined concrete will be obtained from Eq. (11) where $(f'_{cc})_{curve}$ can be read from Fig. 15.

$$f'_{cc} = f'_{cc}(E_{frp}) \times C(d) \times C(h) \times C(t) \times C(\varepsilon_{rup}) \times C(f'_c) \tag{11}$$

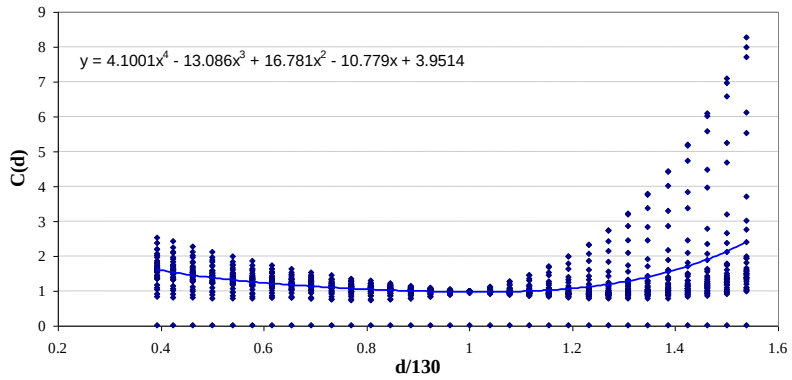

Fig. 21 All data of $C(d)$ and the best fitting curve

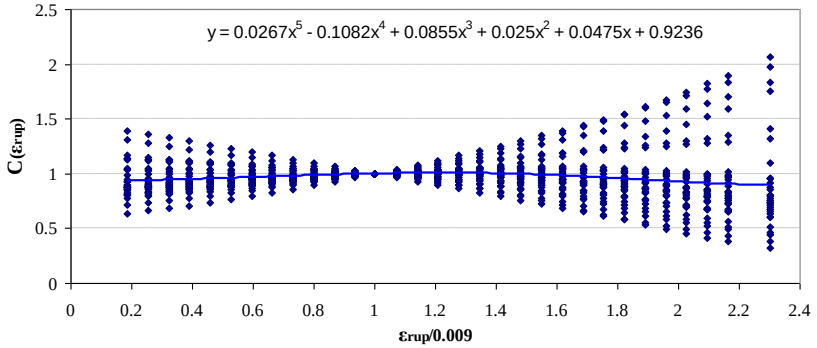

Fig. 22 All data of $C(\varepsilon_{rup})$ and the best fitting curve

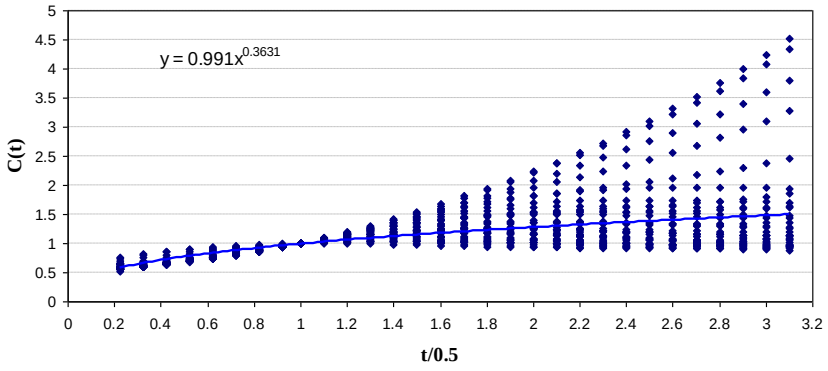

Fig. 23 All data of $C(t)$ and the best fitting curve

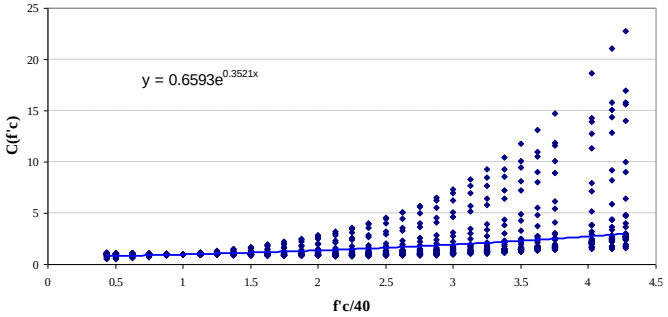

Fig. 24 All data of $C(f'_c)$ and the best fitting curve

6.1 Verification against experimental values and empirical models

Considering the whole data from experimental database, the proposed ANN model is compared with experimental data and the five existing models in Figs. 25 and 26. It can be seen from Fig. 25 that there is relatively good correlation between experimental results and the predicted values by ANN formula.

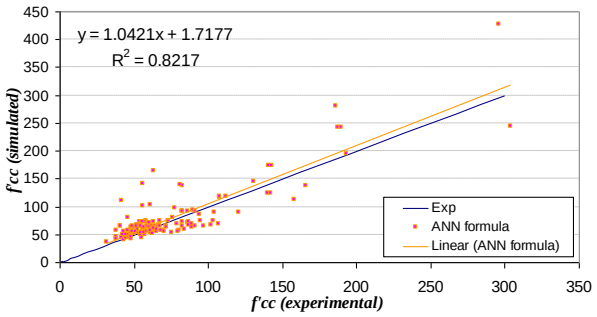

Fig. 25 Correlation between experimental data and predicted values by ANN formula

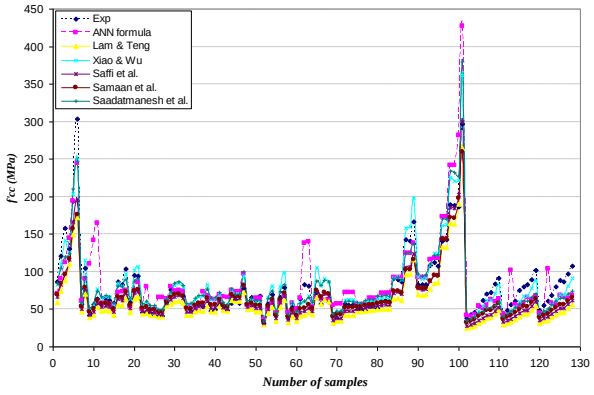

Fig. 26 Comparison of experimental, analytical and ANN formula trends

Moreover, concentrating on Fig. 25, it can be noticed that the values simulated by the ANN model sets spread around the 45° line which implies neither over-estimation nor under-estimation. Also from Fig. 26 it can be easily recognized that the ANN formula closely follows the experimental and analytical trends. Again this is an indication that the network has learned to generalize the information well and reflects good precision in simulation.

7. Conclusions

In the present study, modeling of compressive strength of CFRP-confined concrete cylinders (f'_{cc}) based on gathered experimental data was performed by ANN approach and a formula was derived for prediction based on the input parameters. In this way, a close-form solution based on NN model was obtained which could be easily used to predict f'_{cc}. For this purpose, the optimum NN architecture was obtained by trying different network architectures based on MSE and regression (R) values. The results of the proposed NN model compared to experimental results were found to be quite satisfactory. Moreover, the accuracy of the proposed NN model was compared with several FRP confinement models proposed in literature and found to be far more accurate. The proposed NN model was also presented in explicit form which enables the NN model to be used for practical applications, i.e. this explicit form enables engineers and researchers who are not familiar with NN models to simply use NN-based formula for prediction of f'_{cc} in practice.

References

Ashrafi, H.R., Jalal, M. and Garmsiri, K. (2010), "Prediction of load-displacement curve of concrete reinforced by composite fibers (steel and polymeric) using artificial neural network", *Exp. Syst. Appl.*, **37**(12), 7663-7668.

Berthet, J.F., Ferrier, E. and Hamelin, P. (2005), "Compressive behavior of concrete externally confined by composite jackets, Part A: experimental study", *Constr. Build. Mater.*, **19**(3), 223-232.

De Lorenzis, L., Micelli, F. and La Tegola, A. (2002), "Influence of specimen size and resin type on the behavior of FRP-confined concrete cylinders", Eds. Shenoi, R.A., Moy, S.S.J. and Hollaway, L.C., *Advanced polymer composites for structural applications in construction, proceedings of the first international conference*, London, UK.

Deniaud, C. and Neale, K.W. (2006), "An assessment of constitutive models for concrete columns confined with fiber composite sheets", *Compos. Struct.*, **73**(3), 318-330.

Dias da Silva, V. and Santos, J.M.C. (2001), "Strengthening of axially loaded concrete cylinders by surface composites", Eds. Figueiras, J., Juvandes, L., Faria, R., Marques, A.T., Ferreira, A., Barros, J. and Appleton, J., *Composites in constructions, proceedings of the international conference*, Lisse, Netherland.

Hollaway, L.C. (2004), *Advanced polymer composites for structural applications in construction*, ACIC, Woodhead Publishing.

Harmon, T.G. and Slattery, K.T. (1992), "Advanced composite confinement of concrete", *First international conference on advanced composite materials in bridges and structures*, Sherbrooke, Québec, Canada.

Jalal, M. and Ramezanianpour, A.A. (2012), "Strength enhancement modeling of concrete cylinders confined with CFRP composites using artificial neural networks", *Composites: Part B*, **43**(8), 2990-3000.

Jalal, M., Ramezanianpour, A.A., Pouladkhan, A. and Tedro, P. (2013), "Application of genetic programming (GP) and ANFIS for strength enhancement modeling of CFRP-retrofitted concrete cylinders", *Neural Comput. Appl.*, **23**(2), 455-470.

Karbhari, V.M. and Gao, Y. (1997), "Composite jacketed concrete under uniaxial compression-verification of simple design equations", *J. Mater. Civ. Eng.*, **9**(4), 185-193.
Kono, S., Inazumi, M. and Kaku, T. (1998), "Evaluation of confining effects of CFRP sheets on reinforced concrete members", *Proceedings of the second international conference on composites in infrastructure ICCI'98*, Tucson, Arizona.
Kshirsagar, S., Lopez-Anido, R.A. and Gupta, R.K. (2000), "Environmental aging of fiber reinforced polymer-wrapped concrete cylinders", *ACI Mater. J.*, **97**(6), 703-712.
Lam, L. and Teng, J.G. (2002), "Strength models for fiber-reinforced-plastic-confined concrete", *J. Struct. Eng.*, ASCE, **128**(5), 612-623.
Lam, L., Teng, J.G., Cheng, C.H. and Xiao, Y. (2006), "FRP-confined concrete under axial cyclic compression", *Cement Concrete Res.*, **28**(10), 949-958.
Lee, C. and Hegemier, G.A. (2009), "Model of FRP-confined concrete cylinders in axial compression", *J. Compos. Constr.*, ASCE, **13**(5), 442-454.
Leung, C.K.Y., Ng, M.Y.M. and Luk, H.C.Y. (2006), "Empirical approach for determining ultimate FRP strain in FRP- strengthened concrete beams", *J. Compos. Constr.*, ASCE, **10**(2), 125-138.
Lin, C.T. and Li, Y.F. (2003), "An effective peak stress formula for concrete confined with carbon fiber reinforced plastics", *Can. J. Civ. Eng.*, **30**(5), 882-889.
Matthys, S., Taerwe, L. and Audenaert, K. (1999), "Tests on axially loaded concrete columns confined by fiber reinforced polymer sheet wrapping", *Fourth international symposium on fiber reinforced polymer reinforcement for reinforced concrete structures*, SP-188, American Concrete Institute, Farmington, Michigan, USA.
Matthys, S., Toutanji, H., Audenaert, K. and Taerwe, L. (2005), "Axial load behavior of largescale columns confined with fiber-reinforced polymer composites", *ACI Struct. J.*, **102**(2), 258-267.
Micelli, F., Myers, J.J. and Murthy, S. (2001), "Effect of environmental cycles on concrete cylinders confined with FRP", *Proceedings of CCC2001 international conference on composites in construction*, Porto, Portugal.
Mirmiran, A., Shahawy, M. and Samaan, M. (1999), "Strength and ductility of hybrid FRPconcrete beam-columns", *J. Struct. Eng.*, ASCE, **125**(10), 1085-1093.
Mirmiran, A., Shahawy, M., Samaan, M. and El Echary, H. (1998), "Effect of column parameters on FRP-confined concrete", *J. Compos. Constr.*, ASCE, **2**(4), 175-185.
Miyauchi, K., Inoue, S., Kuroda, T. and Kobayashi, A. (1999), "Strengthening effects of concrete columns with carbon fiber sheet", *Trans. Japan Concrete Inst.*, **21**, 143-150.
Nanni, A. and Bradford, N.M. (1995), "FRP jacketed concrete under uniaxial compression", *Constr. Build. Mater.*, **9**(2), 115-124.
Pessiki, S., Harries, K.A., Kestner, J.T., Sause, R. and Ricles, J.M. (1997), "Axial behavior of reinforced concrete columns confined with FRP jackets", *J. Compos. Constr.*, ASCE, **5**(4), 237-245.
Picher, F., Rochette, P. and Labossiére, P. (1996), "Confinement of concrete cylinders with CFRP", *Proceedings of the first composites in infrastructure ICCI'96*, January, Tucson, Arizona.
Richart, F.E., Brandtzaeg, A. and Brown, R.L. (1928), "A study of the failure of concrete under combined compressive stress", University of Illinois, Engineering Experimental Station, Illinois, USA.
Rochette, P. and Labossiere, P. (2000), "Axial testing of rectangular column models confined with composites", *J. Compos. Constr.*, ASCE, **4**(3), 129-136.
Saadatmanesh, H., Ehsani, M.R. and Li, M.W. (1994), "Strength and ductility of concrete columns externally reinforced with fiber composite straps", *ACI Struct. J.*, **91**(4), 434-447.
Saafi, M., Toutanji, H.A. and Li, Z. (1999), "Behavior of concrete columns confined with fiber reinforced polymer tubes", *ACI Mater. J.*, **96**(4), 500-509.
Samaan, M., Mirmiran, A. and Shahawy, M. (1998), " Model of concrete confined by fiber composites", *J. Struct. Eng.*, ASCE, **124**(9), 1025-1031.
Shahawy, M., Mirmiran, A. and Beitelman, A. (2000), "Test and modeling of carbon-wrapped concrete columns", *Compos. Part B Eng.*, ASCE, **31**(6), 471-480.
Shehata, I.A.E.M., Carneiro, L.A.V. and Shehata, L.C.D. (2002), "Strength of short concrete columns

confined with CFRP sheets", *Mater*. *Struct*., **35**(1), 50-58.
Teng, J.G., Yu, T., Wong, Y.L. and Dong, S.L. (2007), "Hybrid FRP-concrete-steel tubular columns: concept and behavior", *Constr*. *Build*. *Mater*., **21**(4), 846-854.
Toutanji, H.A. (1999), "Stress-strain characteristics of concrete columns externally confined with advanced fiber composite sheets", *ACI Mater*. *J*., **96**(3), 397-404.
Wang, P. and Cheong, K.K. (2001), "RC columns strengthened by FRP under uniaxial compression", Ed. Teng, J.G., *FRP composites in civil engineering, proceedings of the international conference*, Elsevier Science Ltd., Oxford, UK.
Watanabe, K., Nakamura, H., Honda, Y., Toyoshima, M., Iso, M., Fujinaki, T., Kaneto, M. and Shirai, N. (1997), "Confinement effect of FRP sheet on strength and ductility of concrete cylinders under uni-axial compression", *Proceedings of the third international symposium on non-metallic FRP for concrete structures*, Japan.
Xiao, Y. and Wu, H. (2000), "Compressive behavior of concrete confined by carbon fiber composite jackets", *J*. *Mater*. *Civ*. *Eng*., **12**(2), 139-146.

IT